

This work was written as part of one of the author's official duties as an Employee of the United States Government and is therefore a work of the United States Government. In accordance with 17 U.S.C. 105, no copyright protection is available for such works under U.S. Law.

Public Domain Mark 1.0

<https://creativecommons.org/publicdomain/mark/1.0/>

Access to this work was provided by the University of Maryland, Baltimore County (UMBC) ScholarWorks@UMBC digital repository on the Maryland Shared Open Access (MD-SOAR) platform.

Please provide feedback

Please support the ScholarWorks@UMBC repository by emailing scholarworks-group@umbc.edu and telling us what having access to this work means to you and why it's important to you. Thank you.

Geophysical Research Letters

10.1029/2019GL085347

Key Points:

- We present the first quantitative view of how landslide activity may change within High Mountain Asia resulting from changes in extreme precipitation
- We find that the rate of increase in landslide activity at the end of the century is expected to be greatest over areas covered by current glaciers and glacial lakes
- We show how Global Climate Models and satellite observations can be used to model landslide impacts at time scales affected by climate change

Supporting Information:

- Supporting Information S1

Correspondence to:

D. Kirschbaum,
dalia.kirschbaum@nasa.gov

Citation:

Kirschbaum, D., Kapnick, S. B., Stanley, T., & Pascale, S. (2020). Changes in extreme precipitation and landslides over High Mountain Asia. *Geophysical Research Letters*, 47, e2019GL085347.
<https://doi.org/10.1029/2019GL085347>

Received 9 SEP 2019

Accepted 30 JAN 2020

Accepted article online 11 FEB 2020

Changes in Extreme Precipitation and Landslides Over High Mountain Asia

D. Kirschbaum¹ , S. B. Kapnick² , T. Stanley^{1,3} , and S. Pascale⁴ 

¹Hydrological Sciences Laboratory, NASA Goddard Space Flight Center, Greenbelt, MD, USA, ²NOAA/Geophysical Fluid Dynamics Laboratory, Princeton, NJ, USA, ³Universities Space Research Association, Columbia, MD, USA, ⁴Department of Earth System Science, Stanford University, Stanford, CA, USA

Abstract High Mountain Asia is impacted by extreme monsoonal rainfall that triggers landslides in large proportions relative to global distributions, resulting in substantial human impacts and damage to infrastructure each year. Previous landslide research has qualitatively estimated how patterns in landslide activity may change based on climate change scenarios. We present the first quantitative view of potential modulation in future landslide activity over the High Mountain Asia region leveraging a new landslide hazard model and precipitation data from satellite and Global Climate Model sources. In doing so, we find that the rate of increase in landslide activity at the end of the century is expected to be greatest over areas covered by current glaciers and glacial lakes, potentially exacerbating the impacts of cascading hazards on populations downstream. This work demonstrates the potential of Global Climate Models and satellite-based precipitation estimates to characterize landslide hazards at time scales affected by climate change.

Plain Language Summary High Mountain Asia is home to both monsoonal rains and the largest concentration of glaciers outside the North and South Poles. With climate change, heavy rainfall will increase, especially in mountains near glaciers and glacial lakes. This will make landslides more likely and could present new hazards of landslides releasing a wall of water from glacial lakes, impacting communities and infrastructure are located downstream.

1. Introduction

The High Mountain Asia (HMA) region represents a global hot spot for landslide activity due to active seismicity along the Indian and Eurasian plate boundary and extreme seasonal rainfall during the Asian monsoon (Kirschbaum, Stanley, & Zhou, 2015). In this region, landslides damage infrastructure, slow economic development, and cause hundreds to thousands of fatalities each year (Froude & Petley, 2018; Petley et al., 2007). Extreme rainfall from short cloudbursts to prolonged rainfall of several days to weeks is the most significant trigger of landslides (defined for this study as all mass movements from shallow debris flows to complex deep-seated gravitational slides); however, there remain large uncertainties in how climate change may affect landslide activity over HMA in the future. This is further complicated by a dearth of readily available data and models that can be applied at regional scales to quantitatively compare changes between current and future scenarios.

Studies of landslides in a changing climate have included empirical, modeling, or hybrid analyses. An extensive literature review (Gariano & Guzzetti, 2016) evaluated 103 landslide-climate studies around the world, finding significant gaps in research in Asia, South America, and Africa. The study considers previous literature, global hazard models, and landslide databases to characterize potential changes to landslide behavior. They assert that based on the Representative Concentration Pathway (RCP; 2.6 and 8.5) projected by the Intergovernmental Panel on Climate Change (IPCC, 2014), debris flows and shallow landslide hazards over the HMA region may increase due to increases in average surface temperature and precipitation. Studies in Nepal have found increasing trends over the past few decades in both extreme precipitation (Karki et al., 2017) and landslides (Petley et al., 2007); however, characterizing these patterns over all of HMA has been limited by spatiotemporal inconsistencies in precipitation gauges (Shrestha et al., 2000; Winiger et al., 2005) and the sparsity of landslide inventories (Petley et al., 2007). In the context of climate modeling, research highlights the gap between current climate modeling efforts and the application of this information to inform decisions in Nepal (Sharma et al., 2012). The impact of landslide hazards can also have cascading

consequences, such as access to potable water, which is further complicated by uncertainties in water scarcity over HMA resulting from the variability of future precipitation, glacial melt, and population expansion (Immerzeel & Bierkens, 2012). The work here represents a paradigm shift in how we can quantitatively explore the spatiotemporal modulations in potential landslide activity as a result of climate change in this region, particularly in areas already threatened by cascading hazard processes. Combining quantitative data and models provides an innovative opportunity to evaluate future projections against current baselines.

To better characterize potential landslide activity across the region, this work applies a near-global landslide model over HMA called the Landslide Hazard Assessment for Situational Awareness (LHASA) with satellite and Global Climate Model (GCM) precipitation estimates. This allows for the intercomparison of extreme precipitation to provide a baseline from which to evaluate future activity. The incorporation of GCMs with landslides or geomorphic processes has been undertaken in areas within Europe (e.g., Alvioli et al., 2018; Comegna et al., 2013; Dehn & Buma, 1999; Gariano et al., 2017; Rianna et al., 2016; Uzielli et al., 2018), East and South Asia (e.g., Chiang & Chang, 2011; Kim et al., 2015; Komori et al., 2018), and New Zealand (e.g., Schmidt & Glade, 2003). This work is the first study of HMA that applies GCM precipitation estimates within a dynamic landslide model to characterize how changes to extreme precipitation may affect landslide hazard at the end of the century.

2. Data and Methods

2.1. Precipitation Data

Satellite and GCM precipitation data provide a continuous view of the region from which to assess change. Satellite observations from the Tropical Rainfall Measuring Mission (TRMM) Multisatellite Precipitation Analysis (TMPA; Huffman et al., 2010) from 2000 to 2019 enable analysis of extreme rainfall patterns. This work considers the full TMPA record, which has a 0.25-degree, 3-hourly resolution. There are known limitations of TMPA over mountainous regions with significant orographic forcings (Bharti & Singh, 2015), which include the accurate detection of shallow, warm rain processes as well as resolving peak rainfall intensities within storms depending on satellite overpass time. However, TMPA has been found to robustly characterize precipitation patterns over this region over larger space and time windows (Barros et al., 2004; Bookhagen & Burbank, 2006). All product details are provided in Table S1 in the supporting information and further information on how the products are parameterized and used are highlighted in the supporting information S1.

The GCM precipitation estimates are derived from the Geophysical Fluid Dynamics Laboratory forecast-oriented low ocean resolution (FLOR) model (Vecchi et al., 2014). Two configurations of the Geophysical Fluid Dynamics Laboratory FLOR model are considered for this analysis, both of which produce precipitation globally at daily $0.5^\circ \times 0.5^\circ$ horizontal resolution. The first consists of a nudged simulation that includes restored sea surface temperatures to observations and circulation that is nudged to the reanalysis to constrain the model to observed climate from 1982 to 2017 (Nudged GCM). This product generates an output where individual years can be compared directly with satellite products and observed landslides. Additionally, a 30-member ensemble (GCM Ensemble) (Zhang & Delworth, 2018) using historical radiative forcing and projected forcings from the RCP 8.5 are used to produce a fully coupled configuration of FLOR in the present (1961–2000) and future (2061–2100). This provides ample realizations to characterize extreme precipitation in the present and future (1,200 years in each) using the fully coupled GCM directly, instead of requiring extrapolation from a single ensemble member or short observational record of a few decades. The use of a large ensemble reduces uncertainty in the characterization of precipitation extremes (Pascale et al., 2018; van der Wiel et al., 2019), a key objective in understanding changes in landslide risks. Note that all ensemble members use RCP 8.5 and thus sample the upper bound of the RCPs (given that RCP 8.5 has the highest radiative forcing). This may represent the upper bound of increases in precipitation extremes (O'Gorman & Schneider, 2009) within the region in the FLOR model when compared to other RCPs.

The use of several complimentary precipitation data sets is critical to performing our analysis of changing landslide hazards. TMPA precipitation (2007–2015) can be compared with the Nudged GCM (1982–2017) and present climate GCM Ensemble (1961–2000) to assess historical precipitation extremes and validate our use of the GCM in our analysis. The fully coupled GCM Ensemble critically enables the assessment of changes in precipitation extremes caused by climate change over a 100-year period.

2.2. Landslide Model

The precipitation data sets described above are used to force the LHASA model to provide an assessment of present and future landslide hazard. The LHASA model uses a threshold approach to provide near real-time estimates of potential landslide activity by combining landslide susceptibility and precipitation information from TMPA and the Global Precipitation Measurement's multisatellite product called IMERG (Integrated Multi-Satellite Retrievals for Global Precipitation Measurement; Huffman et al., 2018). The landslide susceptibility map is calculated from data sets representing slope, lithology, land cover change, distance to road networks, and distance to fault zones (Stanley & Kirschbaum, 2017). The LHASA model combines a seven-day weighted Antecedent Precipitation Index with global landslide susceptibility information to produce 3-hourly "nowcasts," or maps of potential landslide activity, at a 1-km resolution (Kirschbaum & Stanley, 2018). If the Antecedent Precipitation Index is below the 95th percentile of historical precipitation at that pixel, no nowcast is issued; if the ARI exceeds the 95th percentile, then a "moderate" or "high" nowcast is issued based on the pixel's susceptibility, moderate to high and very high susceptibility, respectively. The model is open source (code is available at <https://github.com/nasa/LHASA>) and subcomponents use freely available data.

An important validation data set for LHASA is NASA's Global Landslide Catalog (GLC), which has been compiled primarily from media reports since 2007. It contains 1,067 landslides in the HMA region from 2007 to 2017. While these include all types of fast-moving landslides, the event's characteristics and mechanisms (e.g., debris flow, mudslide, translational landslide) are rarely specified in the media account. While there are a range of biases impacting the accuracy and completeness of this catalog (Kirschbaum et al., 2010; Kirschbaum, Stanley, & Zhou, 2015), the GLC is a large, open inventory of dated rainfall-triggered landslides within this region (Figure 1). We define the HMA study area using the GLC distribution as a guide and isolating the area with the most frequent landsliding using a slope threshold value of 0.6°, above which the majority of landslides are reported to have occurred. This study region extends from Northern Pakistan to Western Nepal (Figure 1, blue area). To establish a baseline from which to evaluate future landslide activity, LHASA is run retrospectively for the period 2000–2015 using precipitation inputs from both TMPA and a Nudged GCM configuration. Given availability of the GLC, we evaluate the TMPA and Nudged GCM LHASA outputs over the 2007–2015 period with 758 landslides from the GLC.

LHASA performance is assessed with the true positive rate (TPR) and false positive rate (FPR) for the 758 landslides within this region (Table 1). TPR refers to the percentage of landslide reports that are accurately identified by the model, whereas the false positive rate is the estimated percentage of instances where the model indicates that there is landslide potential when no landslide is reported. We call this an estimated FPR because the landslide inventory is incomplete and landslides may have occurred despite no landslides being reported. We evaluate the LHASA outputs from the 30-arcsecond grid cell within which each landslide is located. The one-day TPR represents the proportion of landslides for which a nowcast was issued on the same date. Due to uncertainties in the time of occurrence for many of the landslides (Kirschbaum & Stanley, 2018; Kirschbaum, Stanley, & Zhou, 2015), the TPR is calculated for both the exact date of the reported landslide as well as for three- and seven-day windows surrounding the event. We estimate the FPR by calculating the total number of grid cell-days for which a nowcast was issued and dividing it by the total number of grid cell-days, then subtracting the (negligible) number of true positives.

The LHASA model was also run using the present susceptibility map and future GCM Ensemble daily precipitation from all 30 ensemble members in the periods 1961–2000 and 2061–2100. To estimate the rate of change between the current and future climates, the dates and ensemble members were averaged for the two periods and then the difference was calculated. This provides a metric of percent change of landslide activity over the 2061–2100 time period relative to current conditions. This work is performed for both the winter and summer seasons.

3. Results

3.1. Patterns in Landslides and Extreme Precipitation

Results of the retrospective LHASA analysis predict more historical landslides with TMPA precipitation estimates compared to GCM Nudged inputs, but both versions of the model are sufficiently accurate to describe landslide climatology, or average monthly patterns in landslide activity. The true positive rate ranges from 36% to 68% for TMPA and from 29% to 57% for the Nudged GCM over the one-, three-, and seven-day

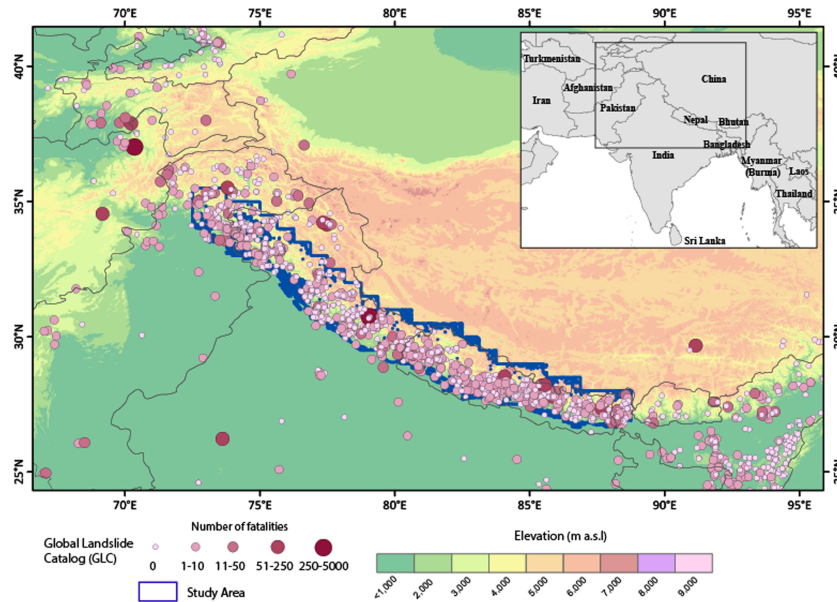


Figure 1. HMA study region, showing the distribution of landslides from NASA's GLC and the study area evaluated.

windows, respectively. We attribute the difference to the lower spatial resolution of the GCM and the fact that the model was designed for use with satellite precipitation estimates. The FPR is nearly identical, which we attribute to the use of a percentile-based precipitation threshold in LHASA. While the model performed better with TMPA precipitation estimates, the GCM precipitation was able to predict landslides with an acceptable level of success, despite having half of the spatial grid resolution. These findings suggest that the GCM precipitation estimates can be used as a proxy for TMPA when applying the model to estimate future potential landslide behavior for this specific case assuming that the results considered in aggregate over time, rather than considered at a specific instance in space and time.

The impact of anthropogenic forcing on future behavior of precipitation extremes over the study region is investigated by comparing the distribution of grid-point daily precipitation (see section 2). Probability distributions of daily precipitation intensities are compared in Figure 2 for TMPA, the Nudged GCM (1982–2017) and GCM Ensemble for the present (1961–2000) and future (2061–2100) periods. Figure 2 further divides this behavior into winter (November to April) and summer (May to October) seasons as HMA precipitation is determined by very different circulation regimes in the two periods, namely, midlatitude westerly disturbances (winter) versus South Asian monsoon (summer). Both the fully coupled GCM Ensemble and Nudged GCM distributions are in good agreement with the TMPA observations for the summer season (Figure 2b). They differ the most (but are still quite similar) at higher precipitation values in the extreme tail when the shorter records of TMPA and the Nudged GCM runs are less useful to assess extreme frequency than the 1,200-year record of the GCM Ensemble (Figures 2, S1, and S2; van der Wiel et al., 2019). The differences in the winter season are more pronounced between TMPA and the FLOR ensemble and are discussed in the supporting information S2. However, we assert that this product is still highly relevant because the majority of landslide-triggering precipitation occurs during the summer months when the monsoon is dominant. This gives us confidence in the use of FLOR to project future extreme rainfall characteristics. The frequency of high-intensity grid-point daily precipitation in HMA is consistently projected to increase in the future, with the most significant increase in very high precipitation intensities (>20 mm/day) in the summertime monsoon season (Figures 2 and S1–S3).

3.2. Future Patterns in Landslide Hazard and Exposure

Results from the future GCM Ensemble suggest that intense precipitation (greater than 20 mm/day) will increase in frequency, which may affect landslide activity across the study region. When comparing the current and future potential landslide activity from LHASA simulations using the GCM, the rate differences

Table 1

LHASA Performance Is Assessed With the True Positive Rate (TPR) and False Positive Rate (FPR) for the 758 Landslides Within This Region

LHASA nowcasts	moderate	One-day TPR	Three-day TPR	Seven-day TPR	FPR
GCM 2007–2015		29%	42%	57%	4.3%
TMPA 2007–2015		36%	55%	68%	4.2%

Note. The TPR is assessed at three temporal windows to account for uncertainty in the reported date of the landslide occurrence. The nowcasts are compared with the reported landslides at the day of the reported event (one day), one day before to one day after the event (three days), and three days before and after the event (seven days) window.

between these two periods reveal a moderate increase in landslide potential over the twenty-first century (Figure 3). However, we found that this increase is not uniform. A few locations (e.g., near Udhampur, India and west of Pokhara, Nepal) show a minor decrease, while the region near the China-Nepal border in the transition zone between the Himalayan Mountains and Tibetan Plateau shows the greatest increases in potential landslide activity (30–70%). While an increase was also observed in much of Tibet, this signal was due to a low precipitation baseline in the twentieth century.

The largest changes to potential landslide activity are expected during the summer months when the monsoon brings in the majority of the extreme rainfall within this region (Figure S3). While this area is not densely populated,

it is home to one of the largest concentrations of glaciers and glacial lakes left by retreating glaciers in the world (Zhao et al., 2014). In Figure 3c, the future change in potential landslide activity (black line) is compared to the change at 131 glacial lakes identified in Nepal (red bars; Rounce, Watson, & McKinney, 2017). Results show that within the areas of glacial lakes, potential landslide activity is projected to increase by 20% or more for 128 (98%) of the lakes and 50% or more for 42 (32%) of the lakes.

4. Discussion

While this study suggests that potential landslide activity may change relative to the current period, the potential impact they may have on glacial lakes is contingent on what these features may look like at the end of the century. Given most glacial lakes are delicately set behind earthen moraine dams from retreating glaciers, increases in extreme precipitation suggested by the GCM (primarily as summer rainfall; see supporting information) that lead to increases in landslide activity can set off a cascade of hazards with far-reaching impacts. A landslide entering the glacial lake could create a wave that destabilizes the moraine dam at the lake's outlet, causing a glacial lake outburst flood that could result in downstream flash flooding (Lala et al., 2018; Rounce, Byers, et al., 2017; Yamada & Sharma, 1993). This rapid flooding could inundate communities and infrastructure situated lower down in the river valleys. Additionally, potential increases in landslide activity proximate to these systems of glacial lakes can cause landslide dams that can also fail catastrophically and endanger communities downstream.

Studies have suggested vastly different patterns in glacier behavior that are both regionally and projection-dependent toward the end of the century, indicating that in some areas such as the Karakoram, glaciers may grow or stagnate (Bolch et al., 2012; Kapnick et al., 2014) while in other areas glaciers may be smaller with larger glacial lakes (Cogley et al., 2010). As glaciers retreat into higher slope areas, the lakes will stay in the valleys and expand downward, providing opportunities for hanging glacial termini or hanging glaciers that could also contribute as potential sources for landslides and avalanches to initiate (e.g., Linsbauer et al., 2016). Should the areas of glacial lakes increase, it also may make them more resistant to glacial lake outburst floods since they could have a greater capacity to absorb the energy triggered by the landslide activity depending on the lake level. One potential analog for future conditions of glacier lakes in Nepal may be the Andes, particularly the Peruvian glaciers, where the glaciers are much smaller but can be extremely hazardous as material falls directly from hanging glaciers and mountains directly into the lakes (e.g., Reynolds, 1992; Vilímek et al., 2005). The possibility of increasing the gravitational potential energy into the lake could significantly increase the hazard of a catastrophic breach. Additional considerations are discussed in the supporting information S3. A critical element of the intersection between changing landslide and glacier dynamics and downstream impacts is the human signature on this landscape in terms of infrastructure development (roads, buildings) as well as the impacts to populations such as access to potable water.

To better understand the potential impact on population due to the predicted changes in potential landslide activity, projected population data in the year 2100 were evaluated for five shared socioeconomic pathways, which each represent a different narrative on the changing patterns of population, urbanization, and style of development (Jones & O'Neill, 2016). Population across the five shared socioeconomic pathways is compared to the potential change in landslide activity and results are shown in Figure 4. When considered at the grid cell level, the anticipated changes in exposed populations are most influenced by national-level

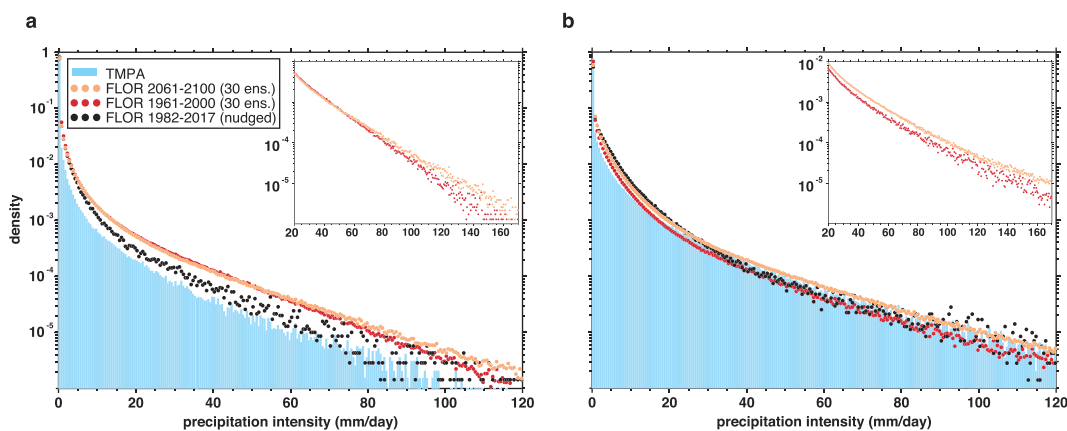


Figure 2. Probability density functions of precipitation over the HMA study region for (a) winter and (b) summer for TMPA (blue), Nudged GCM (black), and GCM 30 member ensemble products (present conditions = red, future conditions = yellow). The inset graph provides additional detail for the higher precipitation intensity values >20 mm/day in the present and future 30-member GCM ensemble simulations. This has also been shown in historical analysis of observed precipitation extremes (Baidya et al., 2008) and regional climate modeling over Nepal (Kulkarni et al., 2013).

changes in population. We show that the majority of the population with this region will experience increased exposure to potential landslide activity, but only 10–13% of the population will be impacted by increased landslide activity greater than 20% (Figure 4). However, most of the variability in exposure to landslide activity is due to differences in projected population. Given that the variability in exposure

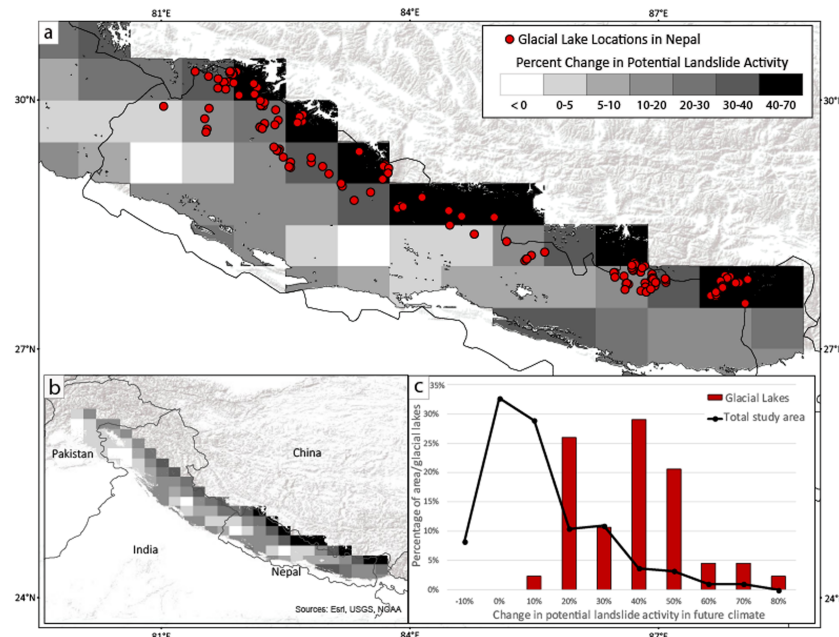


Figure 3. This figure plots the percent change in potential landslide activity comparing the present (1961–2000) and future scenarios (2061–2100), where a positive value indicates an increase in potential landslide activity toward the end of the century. Subplot (a) highlights the spatial pattern over Nepal overlaid with the current locations of 131 glacial lakes, (b) shows the total study area distribution for the full year (Figure S3 shows that these distributions for winter and summer seasons), and (c) plots the distribution of change comparing the potential landslide activity over the study area (black) and the distribution of values at each of the glacial lake in Nepal (red). The categories of change in potential landslide activity are exclusive of the upper value such that the 0–10% bin includes all values from 0 to <10%, 20% bin includes 10% to <20%, etc.

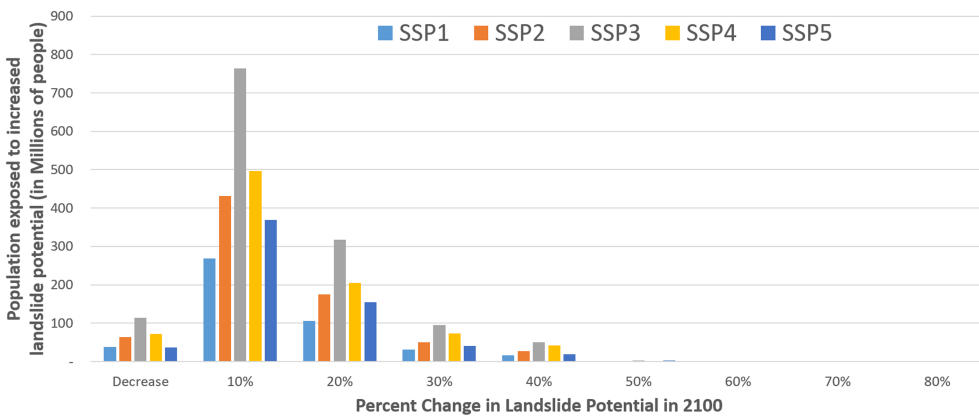


Figure 4. Changes in potential landslide activity between present and future climate scenarios and corresponding changes in exposed population based on the shared socioeconomic pathway (SSP) scenarios in 2100. The categories show the large range of population exposed based on the SPP considered, but also highlights that in general over the study region there will likely be a slight increase (10–20%) in population exposure to landslide hazards at the end of the century.

depends to a large degree on social, behavioral, and political choices, policy makers should consider potential changes to landslide patterns in order to alleviate future risk (Mainali & Pricope, 2017).

5. Conclusions

This synergistic work highlights the potential for merging landslide models with GCM-derived products to better understand and project the impact of extreme precipitation over HMA. Results suggest that increases in extreme precipitation will cause increases in potential landslide activity across the study region, with more pronounced changes in the areas near glacial lakes. The change in local landslide behavior due to potential changing patterns of glaciers and glacial lakes is not explored within this study and represents a large uncertainty in our understanding of how landslides in this region may be impacted or may affect glaciers and glacial lakes in a changing climate. Qualitative comparison of the Intergovernmental Panel on Climate Change projections that consider changes to extreme precipitation (van Oldenborgh et al., 2013) with NASA's global landslide susceptibility map that highlights areas of heightened landslide potential (Kirschbaum, Stanley, & Yatheendradas, 2015), suggest several areas that may experience increases in landslide activity in the future. These include but are not limited to Alaska and Northwest Canada, the U.S. Appalachian mountains, portions of the Andes mountains, Eastern Africa, the Ghats mountain range in India, and central China. While beyond the scope of the current study, the global availability of GCM projections, satellite data, and modeling frameworks will enable new opportunities to evaluate the impacts of changing intense precipitation in these landslide-prone regions and provide more quantitative estimates for how landslide hazards may change and impact communities around the world.

Acknowledgments

The authors would like to thank Xiaosong Yang for running the nudged FLOR simulation and Richard Gudgel for running the 30-member FLOR ensemble. The authors would also like to thank Jeff Kargel, C. Scott Watson, Dan Shugar, and Umesh Haritashya for the insight they provided on glacial lake development and future projections. Support for S.B.K. and S.P. was provided by NASA grant 15-HMA15-0016 and for D.B.K. and T.S. by NASA grant NNX16AT79G. The authors gratefully acknowledge John Lazante and Robert Emberson, who provided comments on the manuscript. Data used in this publication are available at <https://nsidc.org/data/highmountainasia>.

References

- Alvioli, M., Melillo, M., Guzzetti, F., Rossi, M., & Palazzi, E. (2018). Implications of climate change on landslide hazard in central Italy. *Science of the Total Environment*, 630(July). <https://doi.org/10.1016/j.scitotenv.2018.02.315>
- Baidya, S. K., Shrestha, M. L., & Sheikh, M. M. (2008). Trends in daily climatic extremes of temperature and precipitation in Nepal. *Journal of Hydrology and Meteorology*, 5(1), 38–51.
- Barros, A. P., Kim, G., Williams, E., & Nesbitt, S. W. (2004). Probing orographic controls in the Himalayas during the monsoon using satellite imagery. *Natural Hazards and Earth System Sciences*, 4, 29–51. <https://doi.org/10.5194/nhess-4-29-2004>
- Bharti, V., & Singh, C. (2015). Evaluation of error in TRMM 3B42V7 precipitation estimates over the Himalayan region. *Journal of Geophysical Research: Atmospheres*, 120, 12,458–12,473. <https://doi.org/10.1002/2014JD022121>
- Bolch, T., Kulkarni, A., Kaab, A., Huggel, C., Paul, F., Cogley, J. G., et al. (2012). The state and fate of Himalayan glaciers. *Science*, 336(6079), 310–314. <https://doi.org/10.1126/science.1215828>
- Bookhagen, B., & Burbank, D. W. (2006). Topography, relief, and TRMM-derived rainfall variations along the Himalaya. *Geophysical Research Letters*, 33, L08405. <https://doi.org/10.1029/2006GL026037>
- Chiang, S.-H., & Chang, K.-T. (2011). The potential impact of climate change on typhoon-triggered landslides in Taiwan, 2010–2099. *Geomorphology*, 133, 143–151. <https://doi.org/10.1016/j.geomorph.2010.12.028>

- Cogley, J. G., Kargel, J. S., Kaser, G., & van der Veen, C. J. (2010). Tracking the source of glacier misinformation. *Science*, 327(5965), 522–522. <https://doi.org/10.1126/science.327.5965.522-a>
- Comegna, L., Picarelli, L., Buccignani, E., & Mercogliano, P. (2013). Potential effects of incoming climate changes on the behaviour of slow active landslides in clay. *Landslides*, 10(4), 373–391. <https://doi.org/10.1007/s10346-012-0339-3>
- Dehn, M., & Buma, J. (1999). Modelling future landslide activity based on general circulation models. *Geomorphology*, 30(1–2), 175–187. [https://doi.org/10.1016/S0169-555X\(99\)00053-7](https://doi.org/10.1016/S0169-555X(99)00053-7)
- Froude, M. J., & Petley, D. N. (2018). Global fatal landslide occurrence from 2004 to 2016. *Natural Hazards and Earth System Sciences*, 18, 2161–2181. <https://doi.org/10.5194/nhess-18-2161-2018>
- Gariano, S. L., & Guzzetti, F. (2016). Landslides in a changing climate. *Earth Science Reviews*, 162(August 2016), 227–252. <https://doi.org/10.1016/j.earscirev.2016.08.011>
- Gariano, S. L., Rianna, G., Petracci, O., & Guzzetti, F. (2017). Assessing future changes in the occurrence of rainfall-induced landslides at a regional scale. *Science of the Total Environment*, 596–597, 417–426. <https://doi.org/10.1016/j.scitotenv.2017.03.103>
- Huffman, G. J., Adler, R. F., Bolvin, D. T., & Nelkin, E. J. (2010). The TRMM Multi-satellite Precipitation Analysis (TMPA). In F. Hossain & M. Gebremichael (Eds.), *Satellite Rainfall Applications for Surface Hydrology* (pp. 3–22). Dordrecht: Springer Verlag.
- Huffman, G. J., Bolvin, D. T., Braithwaite, D., Hsu, K., Joyce, R. J., & Xie, P. (2018). Algorithm Theoretical Basis Document (ATBD) for NASA Global Precipitation Measurement (GPM) Integrated Multi-satellite Retrievals for GPM (IMERG) v5.2. Retrieved from https://pmm.nasa.gov/sites/default/files/document_files/IMERG_ATBD_V5.2_0.pdf
- Immerzeel, W. W., & Bierkens, M. F. P. (2012). Asia's water balance. *Nature Geoscience*, 5, 841. <https://doi.org/10.1038/ngeo1643>
- IPCC (2014). In C. B. Field, V. R. Barros, D. J. Dokken, J. J. Mach, M. D. Mastrandrea, T. E. Bilir, M. Chatterjee, K. L. Ebi, Y. O. Estrada, R. C. Genova, B. Girma, E. S. Kissel, A. N. Levy, S. MacCracken, P. R. Mastrandrea, & L. L. White (Eds.), *Climate change 2014: Impacts, adaptation, and vulnerability. Part A: Global and sectoral aspects. Contribution of Working Group II to the Fifth Assessment Report of the Intergovernmental Panel on Climate Change* (p. 1132). Cambridge, UK and New York: Cambridge University Press.
- Jones, B., & O'Neill, B. C. (2016). Spatially explicit global population scenarios consistent with the shared socioeconomic pathways. *Environmental Research Letters*, 11(8). <https://doi.org/10.1088/1748-9326/11/8/084003>
- Kapnick, S. B., Delworth, T. L., Ashfaq, M., Malyshev, S., & Milly, P. C. D. (2014). Snowfall less sensitive to warming in Karakoram than in Himalayas due to a unique seasonal cycle. *Nature Geoscience*, 7, 834. <https://doi.org/10.1038/ngeo2269>
- Karki, R., Hasson, S., Schickhoff, U., & Scholten, T. (2017). Rising precipitation extremes across Nepal. *Climate*, 5(4), 1–26. <https://doi.org/10.3390/cl5010004>
- Kim, H. G., Lee, D. K., Park, C., Kil, S., Son, Y., & Park, J. H. (2015). Evaluating landslide hazards using RCP 4.5 and 8.5 scenarios. *Environmental Earth Sciences*, 73(3), 1385–1400. <https://doi.org/10.1007/s12665-014-3775-7>
- Kirschbaum, D., & Stanley, T. (2018). Satellite-based assessment of rainfall-triggered landslide hazard for situational awareness. *Earth's Future*, 6(3). <https://doi.org/10.1002/2017EF000715>
- Kirschbaum, D. B., Adler, R., Hong, Y., Hill, S., & Lerner-Lam, A. (2010). A global landslide catalog for hazard applications: Method, results, and limitations. *Natural Hazards*, 52(3), 561–575. <https://doi.org/10.1007/s11069-009-9401-4>
- Kirschbaum, D. B., Stanley, T., & Yatheendradas, S. (2015). Modeling landslide susceptibility over large regions with fuzzy overlay. *Landslides*, 13(3), 485–496. <https://doi.org/10.1007/s10346-015-0577-2>
- Kirschbaum, D. B., Stanley, T., & Zhou, Y. (2015). Spatial and temporal analysis of a global landslide catalog. *Geomorphology*, 249, 4–15. <https://doi.org/10.1016/j.geomorph.2015.03.016>
- Komori, D., Rangsiwanichpong, P., Inoue, N., Ono, K., Watanabe, S., & Kazama, S. (2018). Distributed probability of slope failure in Thailand under climate change. *Climate Risk Management*, 20, 126–137. <https://doi.org/10.1016/j.crm.2018.03.002>
- Kulkarni, A., Patwardhan, S. K. K. K., Kumar, K. K., Ashok, K., & Krishnan, R. (2013). Projected climate change in the Hindu Kush-Himalayan region by using the high-resolution regional climate model PRECIS. *Mountain Research and Development*, 33(2), 142–151.
- Lala, J. M., Rounce, D. R., & McKinney, D. C. (2018). Modeling the glacial lake outburst flood process chain in the Nepal Himalaya: reassessing Imja Tsho's hazard. *Hydrology and Earth System Sciences*, 22, 3721–3737. <https://doi.org/10.5194/hess-22-3721-2018>
- Linsbauer, A., Frey, H., Haeberli, W., Machguth, H., Azam, M. F., & Allen, S. (2016). Modelling glacier-bed overdeepenings and possible future lakes for the glaciers in the Himalaya–Karakoram region. *Annals of Glaciology*, 57(71), 119–130. <https://doi.org/10.3189/2016AoG71A627>
- Mainali, J., & Pricope, N. G. (2017). High-resolution spatial assessment of population vulnerability to climate change in Nepal. *Applied Geography*, 82, 66–82. <https://doi.org/10.1016/J.APGEOG.2017.03.008>
- O'Gorman, P. A., & Schneider, T. (2009). The physical basis for increases in precipitation extremes in simulations of 21st-century climate change. *Proceedings of the National Academy of Sciences*, 106(35), 14,773–14,777. <https://doi.org/10.1073/pnas.0907610106>
- Pascale, S., Kapnick, S. B., Bordoni, S., & Delworth, T. L. (2018). The influence of CO₂ forcing on North American monsoon moisture surges. *Journal of Climate*, 31(19), 7949–7968. <https://doi.org/10.1175/JCLI-D-18-00071>
- Petley, D. N., Hearn, G. J., Hart, A., Rosser, N. J., Dunning, S. A., Oven, K., & Mitchell, W. A. (2007). Trends in landslide occurrence in Nepal. *Natural Hazards*, 43, 23–44. <https://doi.org/10.1007/s11069-006-9100-3>
- Reynolds, J. M. (1992). The identification and mitigation of glacier-related hazards: Examples from the Cordillera Blanca, Peru. In *Geohazards* (pp. 143–157). Dordrecht, Netherlands: Springer. https://doi.org/10.1007/978-94-009-0381-4_13
- Rianna, G., Comegna, L., Mercogliano, P., & Picarelli, L. (2016). Potential effects of climate changes on soil-atmosphere interaction and landslide hazard. *Natural Hazard*, 84(2), 1487–1499. <https://doi.org/10.1007/s11069-016-2481-z>
- Rounce, D., Watson, C., & McKinney, D. (2017). Identification of hazard and risk for glacial lakes in the Nepal Himalaya using satellite imagery from 2000–2015. *Remote Sensing*, 9(7). <https://doi.org/10.3390/rs9070654>
- Rounce, D. R., Byers, A. C., Byers, E. A., & McKinney, D. C. (2017). Brief communication: Observations of a glacier outburst flood from Lhotse Glacier, Everest area, Nepal. *The Cryosphere*, 11(1), 443–449. <https://doi.org/10.5194/tc-11-443-2017>
- Schmidt, M., & Glade, T. (2003). Linking global circulation model outputs to regional geomorphic models: A case study of landslide activity in New Zealand. *Climate Research*, 25(2), 135–150. <https://doi.org/10.3354/cr025135>
- Sharma, S., Gaillard, J.-C., Jaboyedoff, M., Sudmeier-Rieux, K., & Dubois, J. (2012). Chapter 7 Floods, landslides, and adapting to climate change in Nepal: What role for climate change models? In *Climate Change Modeling For Local Adaptation In The Hindu Kush-Himalayan Region* (Vol. 11, pp. 119–140). Bingley: Emerald Group Publishing Limited. [https://doi.org/doi:10.1108/S2040-7262\(2012\)0000011013](https://doi.org/doi:10.1108/S2040-7262(2012)0000011013)
- Shrestha, A. B., Wake, C. P., Dibb, J. E., & Mayewski, P. A. (2000). Precipitation fluctuations in the Nepal Himalaya and its vicinity and relationship with some large scale climatological parameters. *International Journal of Climatology*, 20(3), 317–327. [https://doi.org/10.1002/\(SICI\)1097-0088\(20000315\)20:3<317::AID-JOC476>3.0.CO;2-G](https://doi.org/10.1002/(SICI)1097-0088(20000315)20:3<317::AID-JOC476>3.0.CO;2-G)

- Stanley, T., & Kirschbaum, D. B. (2017). A heuristic approach to global landslide susceptibility mapping. *Natural Hazards*, 87(1), 145–164. <https://doi.org/10.1007/s11069-017-2757-y>
- Uzielli, M., Rianna, G., Ciervo, F., Mercogliano, P., & Eidsvig, U. K. (2018). Temporal evolution of flow-like landslide hazard for a road infrastructure in the municipality of Nocera Inferiore (southern Italy) under the effect of climate change. *Natural Hazards and Earth System Sciences*, 18, 3019–3035. <https://doi.org/10.5194/nhess-18-3019-2018>
- van der Wiel, K., Wanders, N., Seltten, F. M., & Bierkens, M. F. P. (2019). Added value of large ensemble simulations for assessing extreme river discharge in a 2 °C warmer world. *Geophysical Research Letters*, 46, 2093–2102. <https://doi.org/10.1029/2019GL081967>
- van Oldenborgh, G. J., Collins, M., Arblaster, J., Christensen, J. H., Marotzke, J., Power, S. B., et al. (2013). IPCC, 2013: Annex I: Atlas of global and regional climate projections. In T. Stocker, D. Qin, G.-K. Plattner, M. Tignor, S. K. Allen, J. Boschung, et al. (Eds.), *Climate Change 2013: The Physical Science Basis. Contribution of Working Group I to the Fifth Assessment Report of the Intergovernmental Panel on Climate Change* (pp. 1311–1394). Cambridge, UK and New York: Cambridge University Press. Retrieved from https://www.ipcc.ch/site/assets/uploads/2018/02/WG1AR5_AnnexI_FINAL-1.pdf
- Vecchi, G. A., Delworth, T., Gudgel, R., Kapnick, S., Rosati, A., Wittenberg, A. T., et al. (2014). On the seasonal forecasting of regional tropical cyclone activity. *Journal of Climate*, 27(21), 7994–8016. <https://doi.org/10.1175/JCLI-D-14-00158.1>
- Vilimek, V., Zapata, M. L., Klimeš, J., Patzelt, Z., & Santillán, N. (2005). Influence of glacial retreat on natural hazards of the Palcacocha Lake area, Peru. *Landslides*, 2(2), 107–115. <https://doi.org/10.1007/s10346-005-0052-6>
- Winiger, M., Gumpert, M., & Yamout, H. (2005). Karakorum–Hindukush–western Himalaya: Assessing high-altitude water resources. *Hydrological Processes*, 19, 2329–2338. <https://doi.org/10.1002/hyp.5887>
- Yamada, T., & Sharma, C. K. (1993). Glacier lakes and outburst floods in the Nepal Himalaya. *Snow and Glacier Hydrology*, 218. Retrieved from http://hydrologie.org/redbooks/a218/iahs_218_0319.pdf
- Zhang, H., & Delworth, T. L. (2018). Detectability of decadal anthropogenic hydroclimate changes over North America. *Journal of Climate*, 31(7), 2579–2597. <https://doi.org/10.1175/JCLI-D-17-0366.1>
- Zhao, L., Ding, R., & Moore, J. C. (2014). Glacier volume and area change by 2050 in High Mountain Asia. *Global and Planetary Change*, 122, 197–207. <https://doi.org/10.1016/j.gloplacha.2014.08.006>